BES analysis MEMO V2.01, Sep. 29th, 2001

Partial Wave Analysis of $J/\psi \to \phi\pi^+\pi^-$ and ϕK^+K^-

BES Collaboration
L.Y. Dong[1], D.V.Bugg[2], B.S. Zou[1]

1. Institute of High Energy Physics, Beijing 10039, China.
2. Queen Mary, London E1 4NS, United Kingdom.

Abstract

A partial wave analysis is presented of $J/\psi \to \phi\pi^+\pi^-$ and ϕK^+K^- from a sample of 50 million J/ψ triggers in the BES II detector. The $\phi\pi\pi$ data exhibit a strong signal due to $f_0(1370) \to \pi^+\pi^-$ with mass $M = 1325 \pm 27$ MeV and width $\Gamma = 265 \pm 60$ MeV. There is also a definite signal from $f_0(1770) \to \pi^+\pi^-$ with $M = 1775 \pm 16$ MeV, $\Gamma = 295 \pm 45$ MeV. There is little or no corresponding signal due to $f_0(1770) \to K\bar{K}$. This requires that $f_0(1770)$ is distinct from $f_0(1710)$. The $\phi K\bar{K}$ data contain a strong peak due to $f_2'(1525)$. A small shoulder on its upper side may be fitted by interference between $f_0(1500)$ and a weak $f_0(1710)$ signal. The $f_0(980)$ is observed clearly in both sets of data, and parameters of the Flatté formula are well determined: $M = 971 \pm 6$ MeV, $g_1 = 95 \pm 8$ MeV, $g_2/g_1 = 4.3 \pm 0.5$.

1 Introduction

$J/\psi \to \phi\pi^+\pi^-$ and ϕK^+K^- have been studied by the DM2 [1] and MARK III [2] experiments. Figures 1, 2 and 3 show the DM2 and MARK III data for $J/\psi \to \phi\pi^+\pi^-$ and ϕK^+K^- respectively. The $\pi^+\pi^-$ mass spectrum shown in Figures 1(b) and 2 has several interesting features. The dominant signal near 1 GeV is attributed to the $f_0(980)$. Furthermore, one notices a box-like structure between 1.1 and 1.5 GeV and a small signal around 1.75 GeV. Whether the $f_2(1270)$, $f_0(1370)$ or other states contribute to the box-like enhancement is studied here.

The K^+K^- mass spectrum recoiling against the ϕ, and shown in Figures 1(c) and 3, exhibits a threshold enhancement which we will fit with $f_0(980) \to K\bar{K}$. Evidence for the $s\bar{s}$ state $f_2'(1525)$ in the K^+K^- system, produced in association with a ϕ, is also presented in 1(c) and 3. In addition a shoulder at the high-mass side of the $f_2'(1525)$ is evident. It will be shown that this shoulder may be fitted with interference between $f_J(1710)$ and $f_0(1500)$.

Here, we report BES II data on $J/\psi \to \phi\pi^+\pi^-$ and ϕK^+K^-. They show similar features to DM2 and Mark III data. But the BES II data have much the highest statistics, and are therefore the most suitable for partial wave analysis. So additional information from partial wave analysis of BES II data on $J/\psi \to \phi\pi^+\pi^-$ and ϕK^+K^- may be decisive.

2 Event Selection

About 50M J/ψ collected from November 1999 to May 2001 has been used in this analysis. It is about 5000 runs (Run13691-16835 and Run 17209-19149), but only good runs are used by calling the BES program jpsi_runstatus.f

1. Initial Event Selection

   (a) Charged Track Selection Criteria

   - Four charged tracks with zero net charge, $N_{chrg} = 4$, $\sum Q = 0$.
   - Good helix fit for MDC tracks, MFIT = 2 or -19.
   - Transverse momentum $P_{xy} > 60$ MeV/c.
   - Polar angle of each track in the MDC $|cos\theta| < 0.84$.
   - Event vextex: $\mid \sqrt{x_0^2 + y_0^2} \mid \leq 1.5\ cm$; $\mid z_0 \mid \leq 15cm$.

   (b) Photon Selection Criteria

   - Hit in BSC and Layers > 1.
   - $E_\gamma > 80$ MeV.
   - Shower starts before layer 6.
   - The number of shower counter paired hits should be larger than 2.
   - The angle between photon and its nearest charged track is required to be larger than 10°.
   - Angle between the cluster entering and going through BSC should be less than 20°.

   The correction of energy and error matrix for neutral track have been done by calling the BES program ncor.f

   (c) π, K identification:

   The TOF and dE/dX information are used to identify π and K; we define:

$$\chi_{TOF}(i) = \frac{TOF_{measured} - TOF_{expected-i}}{\sigma_{TOF-i}},$$

$$\chi_{dE/dX}(i) = \frac{PHMP_{measured} - PHMP_{expected-i}}{\sigma_{PHMP-i}},$$

where, $i = \pi, K$ and p; TOF is Time of Flight; $PHMP$ is the Most Probable Pulse Height from the truncated mean.

The TOF and dE/dX correction have been done by calling the BES program toffsig.f and dedxcorr.f

- To identify a pion, it is required that
  when $P \leq 0.75$ GeV/c^2,
  $\mid \chi_{TOF}(\pi) \mid < \mid \chi_{TOF}(K) \mid$, $\mid \chi_{TOF}(\pi) \mid < \mid \chi_{TOF}(p) \mid$,
  $\mid \chi_{TOF}(\pi) \mid < 3.0$;
  or
  $\mid \chi_{dE/dX}(\pi) \mid < \mid \chi_{dE/dX}(K) \mid$, $\mid \chi_{dE/dX}(\pi) \mid < \mid \chi_{dE/dX}(p) \mid$,
  $\mid \chi_{dE/dX}(\pi) \mid < 9.0$.
  If a track satisfies one of the above conditions, $ID = 4$ (pion).
- To identify a kaon, it is required that
  when $P \leq 0.75$ GeV/c^2,
  $\mid \chi_{TOF}(K) \mid < \mid \chi_{TOF}(\pi) \mid$, $\mid \chi_{TOF}(K) \mid < \mid \chi_{TOF}(p) \mid$,
  $\mid \chi_{TOF}(K) \mid < 3.0$;
  or
  $\mid \chi_{dE/dX}(K) \mid < \mid \chi_{dE/dX}(\pi) \mid$, $\mid \chi_{dE/dX}(K) \mid < \mid \chi_{dE/dX}(p) \mid$,
  $\mid \chi_{dE/dX}(K) \mid < 9.0$.
  If a track satisfies one of the above conditions, $ID = 5$ (kaon).
- If a track was identified as a proton, $ID = 6$ (proton).
- If a track does not have TOF and dE/dX information,
  or cannot be identified as π,K, or p, $ID = 7$ (unknown).

The confidence level is also used to identify π and K; we define:

$$PROB(i) = PROB(\chi^2_{TOF}(i) + \chi^2_{dE/dX}(i), 2);$$

If we only have TOF information, then

$$PROB(i) = PROB(\chi^2_{TOF}(i), 1);$$

If we only have dE/dX information, then

$$PROB(i) = PROB(\chi^2_{dE/dX}(i), 1);$$

where, $i = \pi, K$ and p.

- To identify a pion, it is required that,
  $PROB(\pi) > PROB(K)$ and $PROB(\pi) > PROB(p)$.
  If a track satisfies the above condition, $WID = 4$ (pion).
- To identify a kaon, it is required that,
  $PROB(K) > PROB(\pi)$ and $PROB(K) > PROB(p)$.
  If a track satisfies the above condition, $WID = 5$ (kaon).

- To identify a proton, it is required that,
  $PROB(p) > PROB(\pi)$ and $PROB(p) > PROB(K)$.
  If a track satisfies the above condition, $WID = 6$ (proton).
- If a track does not have TOF and dE/dX information,
  or cannot be identified as π,K, or p, $WID = 7$ (unknown).

We use ID to identify π or K. If $ID = 7$, then we use WID to identify π or K. The track which is identified as K must have $PROB(K) > 1\%$; the track which is identified as π must have $PROB(\pi) > 1\%$.

(d) Event Sample Selection Criteria

- The number of neutral clusters is required to be up to ten. and the number of photons which were identified by (b) is required to be less than five.
- For $J/\psi \to K^+K^-\pi^+\pi^-$ initial event selection, it is required that in all cases, one kaon and one pion must be identified unambiguously by (c); whenever the other kaon and pion are ambiguous, all the possibilities are submitted to the following 4-C kinematic fits, $\gamma\gamma 2K2\pi$, $\gamma 2K2\pi$ and $2K2\pi$; only the highest probability: $PROB(\chi^2_{4C}) \times PROB(K^+) \times PROB(K^-) \times PROB(\pi^+) \times PROB(\pi^-)$ are retained; $\chi^2(J/\psi \to K^+K^-\pi^+\pi^-)$ is required to be less than 50.
- For $J/\psi \to K^+K^-K^+K^-$ initial event selection, it is required that $\chi^2(J/\psi \to K^+K^-K^+K^-) < 50$.

2. Final Event Selection

- χ^2 of 4C fit is required to be less than 10.
- ϕ selection:
  it is required that at least one K must be identified and $PROB(K) > 1\%$, $| M_{K^+K^-} - M_\phi |< 15$ MeV.
- For $J/\psi \to \phi\pi^+\pi^-$ channel, it is required that at least one π must be identified and $PROB(\pi) > 1\%$.
- For $J/\psi \to \phi K^+K^-$ channel, it is required that at least one K outside the ϕ must be identified and $PROB(K) > 1\%$.

In the final event sample, after background subtraction, there are 4857 $J/\psi \to \phi\pi^+\pi^-$ events and 3250 $J/\psi \to \phi K^+K^-$. The branching ratios for production of $\phi\pi\pi$ and $\phi K\bar{K}$ are determined allowing for the detection efficiencies for the two channels and correcting for unobserved charge states. Results are:

$$BR(J/\psi \to \phi\pi\pi) = (1.04 \pm 0.02 \pm 0.09) \times 10^{-3}$$

$$BR(J/\psi \to \phi K\bar{K}) = (1.34 \pm 0.03 \pm 0.12) \times 10^{-3}.$$

Here, the relative systematic error for the total number of $/\psi$ is about 7.3% [3], The main cuts (such as χ^2, $PROB(K)$, $PROB(\pi)$, $\mid M_{KK} - M_\phi \mid$, etc.) give rise to about 5% relative systematic error. Then the total relative systematic error is 9%. These agree within the errors with the earlier determinations by DM2 [2], $(1.17 \pm 0.045 \pm 0.18) \times 10^{-3}$ for $\phi\pi\pi$ and $(1.48 \pm 0.08 \pm 0.21) \times 10^{-3}$ for $\phi K\bar{K}$, but are somewhat more accurate.

Figure 4(a) shows the K^+K^- invariant mass distribution of $J/\psi \to K^+K^-\pi^+\pi^-$; the strong signal of ϕ is seen. The $\pi^+\pi^-$ mass spectrum recoiling against the ϕ, shown in Figure 4(b), is obtained by performing a cut on the K^+K^- invariant mass of Figure 4(a): $\mid M_{K^+K^-} - M_\phi \mid < 15$ MeV. Figure 4(c) shows the K^+K^- invariant mass distributions with invariant mass closest to the ϕ mass in $J/\psi \to K^+K^-K^+K^-$; a strong ϕ signal is seen. The K^+K^- mass spectrum recoiling against the ϕ, shown in Figure 4(d), is obtained by performing a cut on the K^+K^- invariant mass of Figure 4(c): $\mid M_{K^+K^-} - M_\phi \mid < 15$ MeV. Figure 5 shows the efficiency for (a) $J/\psi \to \phi\pi^+\pi^-$ and (b) $J/\psi \to \phi K^+K^-$ as functions of $\pi^+\pi^-$ or K^+K^- mass. Figures 6(a) and (c) show the Dalitz plots for $J/\psi \to \phi\pi^+\pi^-$ and $J/\psi \to \phi K^+K^-$ respectively.

The backgrounds to $J/\psi \to \phi\pi^+\pi^-$ and $J/\psi \to \phi K^+K^-$ can be estimated from the sideband from 1.045 to 1.09 GeV in K^+K^- mass of Figures 4(a) and (c). Assuming that background follows a phase space distribution against $K\bar{K}$ mass, the background under the ϕ is 19.0% for $\phi\pi^+\pi^-$ and 6.0% for ϕK^+K^-.

3 Comment on the two halves of the data set

We have looked at the two data sets and see no significant differences between them. Complete PWA have been made (a) to the first data set, (b) to the whole data set. There are negligible changes to results of the PWA from both (a) and (b), despite the fact that (b) increases the data sample by ~ 10 percent in the second set of data. This is illustrated in the following figure 7.

4 Analysis Method

1. The decays $J/\psi \to \phi\pi^+\pi^-$ and ϕK^+K^- are described in terms of a chain of two body processes.

$$
\begin{aligned}
J/\psi \to \phi\ X & \\
&\hookrightarrow \pi^+ \ + \ \pi^- \\
&\hookrightarrow K^+ \ + \ K^-
\end{aligned}
$$

$$
\begin{aligned}
J/\psi \to \phi\ X & \\
&\hookrightarrow K^+ \ + \ K^- \\
&\hookrightarrow K^+ \ + \ K^-
\end{aligned}
$$

2. Formulae used in the fit:

   - The differential cross section is given by:

$$\frac{d\sigma}{d\Phi} = \mid A_{total} \mid^2 + \sigma_{bg},$$

   - The total amplitude is defined as a coherent sum over the amplitudes due to all possible intermediate states,

$$\frac{d\sigma}{d\Phi} = \mid A^{0+} + A^{2+} + A^{4+} + \cdots \mid^2 + BG;$$

   here BG is the background term.
   Each amplitude can be written in the form

$$\begin{aligned} A^{0+}_{1370}(\pi^+\pi^-) &= a_1 e^{ib_1} BW_{f_0(1370)} < \pi^+\pi^- 0^+ 0|0 >, \\ A^{0+}_{1370}(K^+K^-) &= a'_1 e^{ib'_1} BW_{f_0(1370)} < K^+K^- 0^+ 0|0 >, \\ &\cdots\cdots\cdots\cdots\cdots\cdots\cdots, \end{aligned}$$

   where $BW(s) = \frac{M\Gamma}{s - M^2 + iM\Gamma}$, and the notation $< yzJ^p\ell|S >$ describes the partial wave amplitude.

3. Maximum Likelihood Method

   - The probability density function $f(x, \alpha)$ with x_i as a set of independently measured quantities and α as a set of unknown parameters is given by

$$f(x, \alpha) = \frac{d\sigma}{d\Phi}/\sigma,$$

   where $\sigma = \int \frac{d\sigma}{d\Phi} d\Phi$ is the integrated cross section.
   - A fit is made to the data in order to maximize the value of

$$\mathcal{L} = \prod_{i=1}^{N_{event}} f(x, \alpha).$$

   In practice, $S = -\ln \mathcal{L}$ is minimized in the fit.

$$\ln \mathcal{L} = \sum_{i=1}^{N_{event}} \frac{d\sigma}{d\Phi} - \ln \sigma.$$

4. Monte Carlo Integration

- The integrated cross section σ is calculated by Monte Carlo integration

$$\begin{aligned}\sigma &= \int \frac{d\sigma}{d\Phi} d\Phi \\ &= \frac{1}{N'} \sum_{i=1}^{N'} \Big(\mid A_{total} \mid^2 + BG \Big) ,\end{aligned}$$

where N' is the number of Monte Carlo events.

5 Further technical details of the analysis

Amplitudes for each partial wave are written in terms of Lorentz invariant tensors. A notation which will be needed below (and is used in all our work on J/ψ decays) concerns orbital angular momenta. For the production process $J/\psi \to \phi + X$, the orbital angular momentum is denoted by ℓ. The orbital angular momentum in the decay of X to $\pi\pi$ is denoted by L. The amplitudes for the production process are constructed by combining spins of f_0 (or f_2) and the ϕ to make overall $S = 0$, 1 or 2. The possibilities are as follows.

For $J/\psi \to \phi + f_0$, $\ell = 0$ and 2 are allowed. For $\ell = 0$, $S = 0$; for $\ell = 2$, $S = 2$. For $J/\psi \to \phi + f_2$, the possibilities are $\ell = 0$, 2 or 4. For $\ell = 0$, $S = 2$. For $\ell = 2$, S may be 0, 1 or 2. For $\ell = 4$, $S = 2$.

So there are eventually 2 amplitudes describing production of the f_0 and five describing production of f_2. Blatt-Weisskopf centrifugal barriers are included for both production and decay using a radius of 0.8 fm. These are needed for production as well as decay, since the ϕ interacts over a radius of order 0.8 fm. [This is different to $J/\psi \to \gamma X$, where the interaction is of very short range, because the photon has no size and the c quark is heavy]. We find that the $\ell = 4$ amplitude for production of f_2 is negligibly small, probably because of the strong centrifugal barrier.

The line-shape of the ϕ is not fitted, since it is much less than the experimental resolution. There is a second reason. Where a background subtraction is used, it is necessary to treat the sidebin events in the same way as data events; there is no narrow ϕ signal in the sidebins.

The angular dependence of the decay process $\phi \to K^+K^-$ is however included in the amplitudes. This is very important. It turns out that angular correlations between decays of ϕ and f_J are very sensitive to J, and isolate $f_2(1270)$, $f_2'(1525)$ and $f_0(1770)$ very clearly in the analysis.

The final fit is made to both channels $\phi\pi^+\pi^-$ and ϕK^+K^- simultaneously. This combined fit ensures that both channels are fitted with resonances having the same mass and width. It also ensures that relative magnitudes of $\ell = 0$ and $\ell = 2$ production of each resonance are the same in both channels. Branching ratios of each resonance between $K\bar{K}$ and $\pi\pi$ are loosely constrained to be consistent with earlier determinations listed by the PDG.

The acceptance, given by the Monte Carlo simulation, is included in the maximum likelihood fit. All figures shown here are uncorrected for acceptance. This acceptance is quite uniform across Dalitz plots before cuts discussed below.

6 Errors on branching ratios

The errors on branching ratios have been determined in two ways: (i) from statistical errors, i.e. the changes in BR when log likelihood changes by 1 standard deviation, (ii) from systematic errors, i.e. the changes when uncertain components in the fit are removed or changed to their limits. The two errors are then combined in quadrature; usually (ii) dominates.

7 Analysis and Results

The essential features of the data for $J/\psi \to \phi\pi^+\pi^-$ are (i) the strong $f_0(980)$ signal, which cuts off rapidly at the $K\bar{K}$ threshold, (ii) a peak $\sim$ 250 MeV wide centred at 1330 MeV, (iii) a small but definite peak at 1770 MeV. It will be shown that $f_0(1500)$ contributes also. It will also be shown that there is a definite $f_2(1270)$ contribution to the lower side of the peak at 1330 MeV.

In $J/\psi \to \phi K^+K^-$, there is a threshold enhancement which can be attributed to $f_0(980) \to K^+K^-$. The major feature is an asymmetric peak at 1525 MeV. This will be fitted to $f_2'(1525)$, but requires also some additional contribution to produce the shoulder observed at a $K\bar{K}$ mass of 1650 MeV.

7.1 Details of the background

Treatment of the background turns out to be important, and has involved a very lengthy study. In order to examine the background, events are selected within sidebin regions of Figures 4(a) and (c) selected in the K^+K^- mass range 1.045 to 1.09 GeV.

The $\phi\pi$ mass distribution for the $\phi\pi^+\pi^-$ sidebin is shown in Figure 8(b). It contains a striking peak at 1500 MeV. In the Dalitz plot for sidebin events, Figure 8(a), a reflection of this band is clearly visible as a horizontal band towards the bottom of the plot. It is responsible for the broad peak centred at 2450 MeV in Figure 8(b). The origin of these peaks needs to be understood in dealing with the background. It turns out that they are due to $K^*(890)$ in the background.

If events from the lower peak of Figure 8(b) are selected in the mass range 1400–1600 MeV, they give the mass projection on to $M(K^+\pi^-)$ and $M(K^-\pi^+)$ shown in Figure 8(e). There is a strong peak due to $K_1^*(890)$. The mass projection on to $M(K^+\pi^+)$ and $M(K^-\pi^-)$ is shown in Fig. 8(f); there is no narrow K^* peak because the charge combinations correspond to isospin 3/2, but there is a broad peak which arises from kinematic cuts, as discussed below. It will now be shown that the $\phi\pi$

peak at 1500 MeV arises from a kinematic correlation between $K^*(890)$ and the spectator kaon selected within the sidebin.

Suppose K^+, K^-, π^+ and π^- are labelled as particles 1,2,3,4. The correlation arises through the well-known relation

$$s_{12} + s_{23} + s_{13} = M_{123}^2 + 2M_K^2 + M_\pi^2. \quad (1)$$

For the K^*, $s_{23} = 0.89^2$ GeV^2. For the sidebin, the mean value of s_{12} is 1.067^2 GeV^2. Because the kaons have relative momentum within the sideband, $s_{13} \simeq 0.89^2$ GeV^2. From equn. (1), one finds a mean value of $M_{123} = 1490$ MeV. This corresponds closely to the position of the $\phi\pi$ peak. An evaluation of the width of the peak requires calculation of the spread in s_{13} corresponding to the relative motion of K^+ and K^- in the sidebin. The algebra is given in Appendix 1. It leads to a predicted width for the $\phi\pi$ peak of 205 MeV, in close agreement with observation.

For events selected as $\phi\pi^+\pi^-$, the $\phi\pi$ mass distribution is shown in Figure 6(b). There is again a peak at a mass of 1460 MeV, definitely slightly lower than for sidebin events. The lower mass arises because s_{12} is lower than for the sidebin. Equn. (1) predicts a $\phi\pi$ peak at 1462 MeV, and the calculation described in the Appendix predicts a width of 145 MeV; both are in close agreement with the data.

The shift in mass and width of the $\phi\pi$ peak between sidebin and data presents an awkward problem of background subtraction. There are three alternative ways of dealing with it. One is to remove events in the $K^*(890)$ peak by a cut from a $K\pi$ mass of 790 to 990 MeV; this removes the 1500 MeV peak in $\phi\pi$ completely, as shown in Figure 6(f). The second method is to make a background subtraction which allows for the calculated shift in mass and width of the peak as closely as possible. The third is to fit K^* events freely in the amplitude analysis and ignore the background subtraction. A full partial wave analysis has been carried through using both of the first two approaches. A more limited study has been carried out with the third method. All give physics results which agree within the errors. The reason for this is that the physics of f_0 and f_2 in the final state is given by diagonal bands in the Dalitz plots of Figures 8(a) and (e). These bands are not strongly affected by fine details of the way in which the background is treated near the vertical and horizontal edges of the Dalitz plot.

The decrease in width of the $\phi\pi$ peak between sidebin and data makes the predicted peak in data correspondingly higher. [The total number of events is conserved, so the product of height x width must be the same for sidebin and data.] Allowing for this, the magnitude of the peak in data is, within errors, in ageement with that predicted from the sidebin. Consequently there is no surviving evidence for any exotic $\phi\pi$ signal. If the explanation given here for the $\phi\pi$ peak is ignored, the peak is fitted well as a $\phi\pi$ state with $J^P = 1^-$. The origin of this result is that the pion in the $K^*(890)$ has $L = 1$. Combining this $L = 1$ with two kaons having zero orbital angular momentum gives $J^P = 1^-$.

The most reliable method of dealing with the $K^*(890)$ background appears to be removing it with a cut, since no simulation is then required of the shift of the $\phi\pi$

peak. The penalty is a loss of statistics of $\sim 25\%$ of events, although many of these are background. The number of surviving $\phi\pi\pi$ events is 3818. Final fits are obtained by this method, but the second method is used to estimate the magnitude of possible systematic errors. The problem with the third method, fitting the $K^*(890)$ peak freely, is that it ignores the physics of the other $K\pi$ pair; so this is likely to be the least reliable method.

One anticipates that a similar problem may exist for $K_2(1430)$ events in the background. The location of the peak predicted in $\phi\pi$ is at 2140 MeV. However, its width is large, $\sim$ 330 MeV for data and $\sim$ 495 MeV for the sidebin, because of the kinematics. It is known from earlier studies of $J/\psi \to K^+K^-\pi^+\pi^-$ that $K_2(1430)$ arises mostly via the final states $K_2(1430)K^*(890)$ and $K_2(1430)(K\pi)_S$, where $(K\pi)_S$ stands for the κ or $K\pi$ S-wave. The first channel is removed by the $K^*(890)$ cut. The second channel is quite weak. Again two methods of dealing with this possible background have been tried. The first is to include $K_2(1420)\kappa$ explicitly into the fit. The second method is to make a simple background subtraction; the peak in $\phi\pi$ is so broad ($\sim$ 330 MeV) that there is negligible difference between sidebin and background. Differences in results between the two methods are small and the second method is the one finally adopted. In Figure 9(b) which shows the resulting fit, there may be a small surplus of events in the $\phi\pi$ mass projection around 2150 MeV, but it cannot be explained by $K_2(1430)$ or $K_0(1430)$.

7.2 The fit to ϕK^+K^-

The $f_2'(1525)$ is prominent in these data, but the peak is asymmetric. If one fits only $f_2'(1525)$, the fitted mass is 1565 MeV and the width 190 MeV. These are considerably larger than values quoted by the PDG, namely $M = 1525 \pm 5$ MeV, $\Gamma = 76 \pm 10$ MeV. This discrepancy and the fact that the peak is asymmetric suggests the presence of a second component on the upper side of the peak.

We therefore fix the mass of $f_2'(1525)$ at the PDG value and allow the width to increase within the error they quote. Then we try adding further components to the fit. There are two likely alternatives. The first is a background process producing $f_0(980)\phi(1680)$; [production with $f_0(980)$ is required in order to conserve C parity]. The second alternative is to include $\phi(1020)f_0(1710)$.

The first alternative gives only a small improvement in log likelihood, since it fails to fit the decay angular distribution predicted for the $f_0(980)$. The second alternative fits naturally. The shoulder at 1650 MeV arises through constructive interference between $f_0(1500)$ and $f_0(1710)$, with a small additional constructive interference from the tail of $f_0(1370)$. The fit is shown in Figure 9; the combined spin 0 intensity is shown in Figure 9(c). The downward shift of the peak of $f_0(1710)$ by 60 MeV is analogous to the shoulder observed at 1430 MeV in $J/\psi \to \gamma\pi^+\pi^-$ [14]. One must remember that Guo found peaks for the $f_0(1710)$ at 1730 MeV in $J/\psi \to \gamma K^+K^-$ and at 1750 MeV in $J/\psi \to \omega K^+K^-$. It appears likely that interferences are again responsible for small shifts in peak positions. The PDG mass for $f_0(1710)$ appears a reasonable average between all three sets of data.

There is one interesting and striking observation concerning $f_2'(1525)$. It is produced strongly with $\ell = 0$ in the production process (as one would expect). It is also produced equally strongly with $\ell = 2$, but dominantly through the amplitude where $\ell = 2$ combines with spin 2 of $f_2'(1525)$ to make overall spin $S = 2$. For the other two amplitudes where $\ell = 2$ combines with spin 2 of $f_2'(1525)$ to make overall spin $S = 0$ or 1, intensites are an order of magnitude smaller than for the case with $S = 2$. In the fit to $f_2(1270)$ in $\phi\pi\pi$ data described in the next section, the same observation is made. There, the intensities are negligible for $\ell = 2$ partial waves where the overall combined spin with $f_2(1270)$ is $S = 0$ or 1.

7.3 The fit to $\phi\pi^+\pi^-$

We shall postpone a discussion of the detailed fit to $f_0(980)$ to a following section. It is easily fitted to the data with small adjustments to standard values for the mass and the coupling to $\pi\pi$ and $K\bar{K}$. An important detail is that the fit to the lower side of the $f_0(980)$ definitely requires a contribution from the broad component of the $\pi\pi$ S-wave amplitude; as a shorthand, this is denoted by σ. It is fitted using the parametrisation of Bugg, Zou and Sarantsev [4]. From their work, the contribution of $\sigma \to K^+K^-$ is known to be very small in ϕK^+K^- data. It is included with an upper limit given by their analysis, but is almost negligible.

A fit to the peak at 1330 MeV in $\phi\pi\pi$ data requires three components: $f_2(1270)$, $f_0(1370)$ and $f_0(1500)$. Angular correlations between decay of the ϕ and decay of the $f_2(1270)$ identify accurately a peak due to $f_2(1270)$. It optimises at $M = 1291 \pm 17$ MeV with width $\Gamma = 159 \pm 19$ MeV. These values are close to PDG values for $f_2(1270)$. For the final fit, PDG values are used.

The main component of the peak comes from $f_0(1370)$. If fitted with a simple Breit-Wigner amplitude of constant width, it optimises at $M = 1325 \pm 27$ MeV with $\Gamma = 265 \pm 60$ MeV. In order to fit the upper side of the peak accurately, some contribution from $f_0(1500)$ is definitely required. This contribution is better defined by the fit to ϕK^+K^- data, where it plays an essential role in fitting the shoulder at 1650 MeV. The result of the combined fit to $\phi\pi\pi$ and ϕK^+K^- data is that the contribution from $f_0(1500)$ is quite accurately determined.

Earlier determinations of the mass and width of $f_0(1370)$ have been subject to fairly large fluctuations. The first observations were in $\pi\pi \to K\bar{K}$ in experiments at ANL [5] [6] and BNL [8]. Peaks called S were observed in all three experiments around a mass of 1300 MeV. From a combined fit to Crystal Barrel data on $\bar{p}p \to 3\pi^0$ and the data on $\pi\pi \to K\bar{K}$, Bugg, Zou and Sarantsev found [4] $M = 1300 \pm 15$ MeV, $\Gamma = 230 \pm 16$ MeV. However, in the Crystal Barrel data the $f_0(1370)$ is not directly visible, but its parameters must be deduced from detailed fitting to the data. Publications of the Crystal Barrel group have reported masses as high as 1390 MeV from 4π data [8]. However, a definite difference in peak position is expected between 2π and 4π data [9]. The phase space for 4π increases extremely rapidly with mass. Modelling this effect, Ref. [9] predicts that the 4π peak will be 50–100 MeV higher than that in 2π. There is therefore no discrepancy between the mass of 1325 MeV found here and Thoma's value of 1390 MeV for the 4π channel.

The peak in Figures 9(a) and (c) is much the clearest observation of $f_0(1370)$ so far. Since some authors have suggested that it does not exist [10], direct verification of its existence is important. A definite resonant phase variation is required with respect to $f_2(1270)$, $f_0(1500)$ and the broad $\sigma \to \pi\pi$ amplitude. Table 1 below shows changes in log likelihood when each component is dropped from the fit and the remainder are re-optimised. For $f_0(1370)$, this change corresponds to an effect greater than 9σ. A fit with $f_2(1270)$ and $f_0(1500)$ alone is not capable of fitting the data accurately.

Channel	Mass (MeV)	Width (MeV)	Fraction $\phi\pi^+\pi^-$(%)	Fraction ϕK^+K^-(%)	ΔS
$f_0(980)$	971 ± 6	see text	26.5	17.5	707
$f_0(1370)$	1325 ± 27	265 ± 60	11.9	6.5	72
$f_0(1500)$	PDG	PDG	12.9	7.6	65
$f_0(1770)$	1775 ± 16	295 ± 45	10.9	-	88
$f_2(1270)$	PDG	PDG	13.2	0.6	167
σ			23.9	4.1	209
$f_2'(1525)$	PDG	82	-	29.8	289
$f_0(1710)$	1700^{+20}_{-40}	200 ± 35	-	9.6	67

Table 1: Parameters of fitted resonances. Branching fractions for each channel after correction for background; their sum differs from 100% because of interferences. Improvements in $S =$ log likelihood.

At high $\pi\pi$ masses, there is a further peak at ~ 1770 MeV. If fitted with spin 0, the fitted mass is $M = 1775 \pm 16$ MeV, $\Gamma = 295 \pm 45$ MeV. These compare well with parameters for $f_0(1770)$ reported from Crystal Barrel data [11], namely $M = 1770 \pm 12$ MeV, $\Gamma = 220 \pm 40$ MeV. Allowing for the number of fitted parameters, $f_0(1770)$ is more than a 10σ signal.

If one tries to fit the 1770 MeV peak with spin 2 instead, log likelihood is worse by 18.2, despite the fact that the fit with spin 2 uses 4 amplitudes compared with 2 for spin 0. Allowing for the number of fitted parameters, the difference is statistically more than a 7σ effect.

There is little phase space for the production of the $f_J(1770)\phi(1020)$ final state. Hence production with $\ell = 2$ is likely to be limited by the centrifugal barrier. A fit with only $\ell = 0$ and $J = 2$ gives a much poorer fit than with $J = 0$, by 94 in log likelihood. It has been observed both here and in fitting ωf_J final states that addition of three further amplitudes with $\ell = 2$ (corresponding to the three allowed helicities for f_2) leads to considerable flexibility in the fit; the four spin 2 amplitudes can simulate the isotropic decay angular distribution of a spin 0 resonance and its production angular distribution. Therefore the difference in log likelihood of 18.2 between spin 2 and spin 0 must be regarded as a lower limit. [Experience elsewhere is that each new fitted amplitude may improve log likelihood by 10–20.] Hence it appears that spin 0 is decisively favoured over spin 2.

There is one further pointer towards spin 0. We remarked above that $f_2'(1525)$ and $f_2(1270)$ are both produced dominantly with overall spin $S = 2$ after one combines ℓ of the production process with spin 2 of the f_2. However, a fit to $f_2(1770)$ behaves quite differently. The intensites with combined spin $S = 0$ or 1 are dominant. Omitting them from the fit, log likelihood is worse by 66.

Further observations of $f_0(1770)$ are summarised in [11]; these include its observation in $J/\psi \to \gamma(4\pi)$ [12] [13]. A radial excitation of $f_0(1370)$ is to be expected in the mass range 1700–1800 MeV; $f_0(1770)$ decaying to $\pi\pi$, $\eta\eta$ and 4π is a good candidate for this radial excitation.

7.4 Fitting $f_0(980)$

The $f_0(980)$ is fitted with the usual Flatté formula [15], [16] :

$$f = \frac{1}{M^2 - s - iM(g_1\rho_1 + g_2\rho_2)}, \qquad (2)$$

where $\rho_{1,2}$ are the phase space factors for $\pi\pi$ and $K\bar{K}$ channels, $\rho_i(s) = \sqrt{1 - m_i^2/4s}$ and $g_{1,2}$ are squares of coupling constants to the two channels. For the $K\bar{K}$ channel, m^2 is taken as the average for K^0 and $K^\pm$, and the algebraic expression for ρ_2 is continued analytically below the $K\bar{K}$ threshold.

From earlier work [4], the ratio g_2/g_1 is known only approximately. The reason for this lies in disagreements between experiments on $\pi\pi \to K\bar{K}$, Ref. 4–6. These experiments differ in absolute normalisation by up to a factor 1.5.

The present data offer the opportunity to determine the ratio g_2/g_1 accurately. This is done by determining the number of events due to $f_0(980) \to \pi\pi$ and $\to K^+K^-$ and comparing with the prediction from the Flatté formula. After making the best fit to the data, the fitted $f_0(980) \to \pi^+\pi^-$ signal is integrated over the mass range from 900 to 1000 MeV. The K^+K^- signal is integrated over the mass range 1.0–1.2 GeV, so as to avoid sensitivity to the tail of the $f_0(980)$ at high mass. The latter integral is given by

$$0.5 \int ds |f(980)|^2 \rho(K^+K^-) \epsilon(K^+K^-) \qquad (3)$$

and the former by

$$\frac{2}{3} \int ds |f(980)|^2 \rho(\pi\pi) \epsilon(\pi^+\pi^-). \qquad (4)$$

Here ϵ_i are detection efficiencies. The numerical factors at the beginning of each expression take into account the facts that (a) there are equal numbers of decays to K^+K^- and $K^0\bar{K}^0$, (b) two-thirds of $\pi\pi$ decays are to $\pi^+\pi^-$ and one third to $\pi^0\pi^0$.

By an iterative process which converges rapidly, the ratio g_2/g_1 is adjusted until the ratio of these two integrals reproduces the fitted numbers of events for ϕK^+K^- and $\phi\pi^+\pi^-$ in the mass ranges described above. The result is

$$g_2/g_1 = 4.3 \pm 0.5. \tag{5}$$

This is a considerable improvement on the earlier determination. Finally, the mass and g_1 are adjusted to achieve the best overall fit to the peak in $\phi\pi^+\pi^-$ data. Values are $M = 971 \pm 6$ MeV, $g_1 = 95 \pm 8$ MeV. These appear to be the best determination up to now of the parameters of $f_0(980)$, mainly because of the improvement in the determination of g_2/g_1. The error in the new determination arises largely from uncertainty in interference in $\phi\pi^+\pi^-$ with the broad σ component.

7.5 Branching ratio of $f_0(1370)$ to K^+K^-

A point of interest is the branching ratio of $f_0(1370)$ between $K\bar{K}$ channels and $\pi\pi$. The WA102 group quotes [18]:

$$\frac{f_0(1370) \to K\bar{K}}{f_0(1370) \to \pi\pi} = 0.46 \pm 0.15 \pm 0.11. \tag{6}$$

A free fit to present data gives

$$\frac{f_0(1370) \to K\bar{K}}{f_0(1370) \to \pi\pi} = 0.38^{+0.30}_{-0.11}, \tag{7}$$

in good agreement with WA102.

Comparable decay branching ratios to $K\bar{K}$ and $\pi\pi$ are also consistent with data on $\pi\pi \to K\bar{K}$. Bugg, Sarantsev and Zou [4] fitted those data together with CERN-Munich data on $\pi\pi$ elastic scattering. In CERN-Munich data, the branching ratio for $f_0(1370) \to \pi\pi$ in restricted to a small value. In order to maximise the signal for $f_0(1370)$ in $\pi\pi \to K\bar{K}$, it is necessary to have branching fractions to $\pi\pi$ and $K\bar{K}$ within a factor 2 of one another. This agrees with the branching ratio found here.

7.6 Branching ratio of $f_0(1500)$ to K^+K^-

The WA102 group finds

$$\frac{f_0(1500) \to K\bar{K}}{f_0(1500) \to \pi\pi} = 0.33 \pm 0.03 \pm 0.07. \tag{8}$$

Crystal Barrel report a somewhat lower value of 0.19 ± 0.07 [19]. However, the Crystal Barrel value has been criticised at conferences by the Obelix group, which finds a value at least a factor 2 larger.

In fitting present data, we constrain the branching ratio to the band of values allowed by Crystal Barrel and WA102. All fits require a $K\bar{K}$ branching ratio towards the top of the range found by WA102. Our conclusion is that the Crystal Barrel branching ratio is definitely too low to fit present data.

7.7 $f_0(1770)$ does not decay to $K\bar{K}$

A striking feature of $f_0(1770)$ is that there is no peak at that mass in ϕK^+K^- data. From analysis of $J/\psi \to \omega K^+K^-$, Guo found a branching ratio $f_0(1710) \to K^+K^-/f_0(1710) \to \pi^+\pi^- = 5.6 \pm 1.7$ [17]. If this ratio is applied to $f_0(1770)$ it predicts an enormous signal in ϕK^+K^- data.

If the $f_0(1770)$ is used to fit the shoulder at 1650 MeV in ϕK^+K^- using mass and width consisent with $\phi\pi\pi$ data, the fit is poor; the mass is too far from the location of the shoulder to give an adequate fit. However, if this poor fit is accepted, the branching ratio $f_0(1770) \to K\bar{K}/f_0(1770) \to \pi\pi$ would be only 0.56 ± 0.10. This is a factor 10 lower than Guo's result [17] and other observations of $f_0(1710)$. Hence there must be two resonances in the mass range 1700–1800 MeV. The $f_0(1710)$ decays dominantly to $K\bar{K}$ and the $f_0(1770)$ is needed to explain present data, plus decays to $\eta\eta$ observed in the Crystal Barrel experiment, plus decays to 4π observed in $J/\psi \to \gamma(4\pi)$.

It is unreasonable to invent a third 0+ meson at 1650 MeV decaying to KK but not pi-pi. In this mass range, there is only room in the quark model for one s-sbar state and one n-nbar radial excitation. These positions are already filled by f0(1710) and f0(1770) respectively. A fit with f0(1650) instead of f0(1710) in no better than with f0(1710), so we consider one should avoid inventing another 0+ resonance in this mass range, in the absence of convincing evidence. It would generate an unnecessary inconsistency with the masses found by Guo in gamma(KK) and omega-KK.

7.8 Branching fractions within each channel

Table 1 shows a summary of fitted resonance masses and widths. It also gives percentage intensities observed for each channel, ignoring interferences between channels. For ϕK^+K^-, they add up to significantly less than 100% because of strong constructive interferences between $f_0(1370)$, $f_0(1500)$ and $f_0(1710)$ in producing the shoulder at 1650 MeV in K^+K^-.

Note that in Table 1, branching fractions to ϕK^+K^- are strongly correlated with those for $\phi\pi^+\pi^-$. In particular, the branching fraction for $f_2(1270)$ is set from $\phi\pi\pi$ using the PDG branching ratio of $f_2(1270)$ between $K\bar{K}$ and $\pi\pi$. The branching fraction of $\sigma \to K^+K^-$ is constrained to the upper limit observed in fitting $\pi\pi \to K\bar{K}$ [11].

The last column of Table 1 shows changes in log likelihood when each channel is removed from the fit and remaining parameters are re-optimised. Allowing for the number of fitted parameters, the significance of the $f_0(1370)$ is over 9σ; that of $f_0(1770)$ is over 10σ.

8 Comment on Analysis in slices of mass

It has been suggested that the analysis should be made in slices of $\pi\pi$ and K^+K^-

mass. This type of analysis was attempted at an early stage but encounters many problems which we now outline.

a) In ϕK^+K^-, the $f_2'(1525)$, which has a very well known mass and width, acts as a strong interferometric signal. In particular, its phase variation with mass helps determined the magnitude and phase of neighbouring 0^+ signals. If one fits the 2^+ signal in the KK mass range 1400-1750 MeV freely, one gets results which destroys the phase information from $f_2'(1525)$. In any one slice, one can only determine magnitudes plus real parts of interferences. If the phase is undetermined, the real parts of interferences can be confused with magnitudes of signals. As a result, the are enormously strong correlations within each slice between phases and magnitudes. Neither is well determined alone; only a correlated piece of information survives.

So the slice analysis must be done in such a way as to preserve the PHASE of the 2^+ component in each slice. This is done by adding a constraint to this phase in every slice.

(b) Similar remarks apply to $f_2(1270)$ in $\phi\pi^+\pi^-$, though the signal is smaller and less useful as an interferometer. Nonetheless, the phase information from the $f_2(1270)$ is a vital ingredient in determining the phase of the 0^+ contribution. Therefore it is again essential to preserve the phase information of the $f_2(1270)$ contribution as a function of mass in the slice analysis. Without this constraint, a slice analysis cannot show that $f_0(1330)$ has a resonant phase variation, since there is nothing for it to interfere with.

(c) In general, the problem with slice analysis is that it allows large and random phase variations from slice to slice. A fundamental constraint in PWA is that amplitudes are analytic functions of s. The slice analysis discards this constraint and produces a result inconsistent with analyticity, therefore definitely inferior. Previous experience is that rejecting the constraint of analyticity throws away much of the available physics.

Even when phase constraints are applied to $f_2'(1525)$ and $f_2(1270)$, insuperable problems remain, as follows.

(d) It is essential in the analysis to constrain the $\sigma \to KK$ branching ratio to be very small, for consistency with data on $\pi\pi \to KK$, where the absolute cross section is known (and small compared with $\pi\pi \to \pi\pi$) [12]. A free fit to $\sigma \to KK$ gives a contribution a factor 10 larger, but with only a small change in log likelihood. The reason is straightforward: adding a broad 0^+ component in KK allows additional unphysical interferences with $f_0(1370)$, $f_0(1500)$ and $f_0(1710)$, giving minor improvements (invisible on graphs) in narrow ranges of mass. The slice fit is unstable against such variations, and gives a result inconsistent with $\pi\pi \to KK$.

(e) Likewise, it is necessary to constrain the branching ratios of $f_0(1330)$ and $f_0(1500)$ between KK and $\pi\pi$ to constant values. Separating the $f_0(1370)$ and $f_0(1500)$ is difficult. In a slice analysis, one cannot distinguish between $f_0(1330)$ and $f_0(1500)$ components. If one fits $\phi\pi\pi$ freely, the tendency is for the $f_0(1370)$ component to become large and swallow $f_0(1500)$. But the $f_0(1500) \to KK$ component is required strongly by ϕKK data. In a free fit to individual slices of mass, the branching ratio for the 0^+ component between K^+K^- and $\pi\pi$ fluctuates wildly; in the mass range around 1500 MeV, the component attributable to $f_0(1500)$ becomes too large for consistency with data from WA102 and Crystal Barrel.

These problems are solved by fitting analytic functions to the data. We find that constraining the branching ratios to values consistent with WA102 implies only a very small penalty in log likelihood of about 10.

8.1 General remark on $\phi\pi\pi$

It is remarkable that $\phi\pi\pi$ data contain large signals due to several states which are predominantly non-strange: $f_2(1270)$, $f_0(1370)$, $f_0(1500)$ and $f_0(1770)$. Direct production of the ϕ should favour its association with $s\bar{s}$ states. This is a long-standing puzzle. We speculate that the basic production process is $J/\psi \to K^*K^*$, where K^* may represent any $K\pi$ resonance. This process is known to be strong [20]. After K^* decays, $K\bar{K}$ pairs may rescatter to ϕ and $\pi\pi$ pairs to f_0 or f_2. The ϕ has a long lifetime and leaves the region of strong interaction before decaying. Following its decay, it is unlikely that kaons rescatter with pions to form K^*.

9 Conclusions

By using both data on $\phi\pi^+\pi^-$ and ϕK^+K^-, we are able to improve the determination of g_2/g_1 for $f_0(980)$: $g_2/g_1 = 4.3 \pm 0.5$. This in turn leads to improvements in g_1 and the mass, which are correlated with g_2 when fitting data.

In the $\phi\pi^+\pi^-$ data, there is a conspicuous signal at $\sim$ 1330 MeV requiring a dominant spin 0 contribution. This is the clearest observation so far of $f_0(1370)$. The $f_2(1270)$ contributes to the lower side of this peak and $f_0(1500)$ to its upper side. The fitted mass and width of $f_0(1370)$ are $M = 1325 \pm 27$, $\Gamma = 290 \pm 45$ MeV.

At high masses, there is a small but definite signal consistent with $f_0(1770) \to \pi^+\pi^-$. For that state, spin 0 is strongly preferred over spin 2, in agreement with Ref. [11].

In ϕK^+K^- data, there is a strong contribution from $f_2'(1525)$. On its upper side, a spin 0 contribution is required and may be fitted with $f_0(1710)$. The decay branching ratio of $f_0(1770)$ between $\pi\pi$ and $K\bar{K}$ is definitely distinct from $f_0(1710)$ observed in ωK^+K^-, hence requiring two resonances in this mass range. The Θ, which is observed dominantly in $K\bar{K}$, may be the $s\bar{s}$ member of the ground-state 0^+ nonet. The $f_0(1770)$ is likely to be the radial excitation of $f_0(1370)$. Both may well be mixed with the 0^+ glueball expected in this mass range.

10 Appendix

This appendix discusses the width to be expected for the $\phi\pi$ peak for sidebin and $\phi\pi\pi$ data.

The basic kinematic relation is equn. (1), repeated here for convenience:

$$s_{12} + s_{23} + s_{13} = M_{123}^2 + 2M_K^2 + M_\pi^2.$$

Firstly we discuss the effect of the natural line-widths of $K^*(890)$ and ϕ. Both are described by Breit-Wigner amplitudes $1/(M^2 - s - iM\Gamma)$. The amplitude describes a pole at $s = M^2 - iM\Gamma$. Equn. (1) may be used to evaluate the effect on the imaginary part of the pole position $M\Gamma$ in the 123 channel:

$$M_{123}\Gamma_{123} = M_\phi\Gamma_\phi + M_{K^*}\Gamma_{K^*} = 1.019417 \times 0.004458 + 0.8961 \times 0.0507\ GeV.$$

The width of the $\phi\pi$ peak arising directly from the widths of ϕ and $K^*(890)$ is only 34 MeV; for any peak arising from ϕ and $K_2(1430)$ it is 75 MeV.

In the first approximation used so far, it is assumed that $s_{13} = s_{23}$. It is necessary to remove this approximation, by allowing for the relative motion of K^+ and K^- in the ϕ.

It is easiest to do the algebra in the rest frame of the ϕ. Figure 12 sketches the kinematics. If $M(\phi\pi_3)$ is fixed, $p_\pi = p_{\pi_3} - p_\phi$ is fixed. Also $p_K = p_{K_2} - p_\phi$ is fixed in the ϕ. It is easy to work out the mass of the 23 combination. If the angle θ is $< 90°$, this mass is reduced by the internal motion of the ϕ. The mass of the 13 combination is increased by an equal perturbation, as shown below.

The algebra is as follows:

$$\begin{aligned} M_{23}^2 &= (E_\pi + E_K)^2 - (p_\pi + p_K\cos\theta)^2 - p_K^2\sin^2\theta \qquad (9) \\ &= M_\pi^2 + M_K^2 + 2E_\pi E_K - 2p_\pi p_K\cos\theta. \end{aligned}$$

If M_{123}^2 is fixed at the value $(M_\pi^2 + M_K^2 + 2E_\pi E_K)$, the perturbation to M_{23}^2 is $-2p_\pi p_K\cos\theta$. The corresponding perturbation to M_{13}^2 is equal and opposite, since $\cos\theta$ simply changes sign.

However, this result is not quite what is required. The mass of $\phi\pi_3^+$ is not really fixed. If the $K^*(890)$ is very narrow, what is really fixed is M_{23}, i.e. the pole position of $K^*(890)$ fixes M_{23}^2 not M_{123}^2. Then, as θ varies, the mass of $\pi\phi$ varies. The mass of the 13 combination changes by twice this amount, since the length of the momentum vector from 1 to 2 is twice the length of that from particle 2 to the centre of mass of the ϕ. The perturbation to M_{13}^2 is then $\Delta = 4p_\pi p_K\cos\theta$.

The value of $\cos\theta$ is uniformly distributed from $\cos\theta = -1$ to $+1$. Correspondingly, M_{13}^2 is also uniformly distributed and so too is that of M_{123}^2. The σ of this distribution is $\Delta^2/3$. So if the distribution is approximated by a Gaussian, $\sqrt{\sigma} = 4p_\pi p_K/\sqrt{3}$. A Gaussian falls to half-height at $1.386\sqrt{\sigma}$. So, for a Lorentz line-shape,

$$M_{123}\Gamma_{123} \simeq 1.386 \times 4p_\pi p_K/\sqrt{3}.$$

Inserting numbers, one finds that the effect on the width of the $\phi\pi$ peak for sidebin events is 203 MeV for events making $K^*(890)$. Adding the natural line-width in quadrature, one gets a full width of 205 MeV. For ϕ events, the calculation of kinematics gives 142 MeV, and adding the natural line width in quadrature increases this to 145 MeV. For events making $K_2(1430)$, the width of the $\phi\pi$ peak for sidebin events is 495 MeV and for ϕ events it is 328 MeV.

References

[1] L. Kopke in : Proc. XXIIIrd Int. Conf. on High Energy Physics (Berkeley, 1986), ed. S. Loken (World Scientific, Singapore, 1987) and Santa Cruz preprint SCIPP 86/74.

[2] A. Falvard et al., Phys. Rev. D38 (1988) 2706.

[3] Fang Shuangshi, Zhu yucan, Determination of total number of J/psi from 4-prong Data.

[4] D.V. Bugg, A.V. Sarantsev and B.S. Zou, Nucl. Phys. B471 (1996) 59.

[5] V.A. Polychronakos et al., Phys. Rev. D19 (1979) 1317; A.D. Martin and E.N. Ozmutlu, Nucl. Phys. B158 (1979(520.

[6] D. Cohen et al., Phys. Rev. D22 (1980) 2595.

[7] A. Etkin et al., Phys. Rev. D25 (1982) 1786.

[8] U. Thoma *Hadron Spectroscopy*, AIP Conf. Proc. 432 (1998) 322.

[9] A.V. Anisovich et al., Nucl. Phys. A690 (2001) 567.

[10] P. Minkowski and W. Ochs, Frascati Physics Series, 15 (1999) 245.

[11] A. Anisovich et al., Phys. Lett. B449 (1999) 154.

[12] D.V. Bugg et al., Phys. Lett. B353 (1995) 378.

[13] J.Z. Bai et al., Phys. Lett. 472 (2000) 207.

[14] BES collaboration, *Further Data on* $J/\psi \to \gamma(K^+K^-)$ *and* $\gamma(\pi^+\pi^-)$, to be submitted to Physics Letters B?

[15] S. Flatté, Phys. Lett. 63B (1976) 224.

[16] B.S. Zou and D.V. Bugg, Phys. Rev. D48 (1993) R3948.

[17] BES collaboration, *Data on* $J/\psi \to \omega(K^+K^-)$ *and* $\omega(\pi^+\pi^-)$, to be submitted to Physics Letters B?

[18] A. Kirk, Nucl. Phys. A663 (2000) 608c.

[19] A. Abele et al., Phys. Rev. D57 (1998) 55.

[20] Particle Data Group (PDG), Euro . Phys. Journ. C15 (2000) 1.

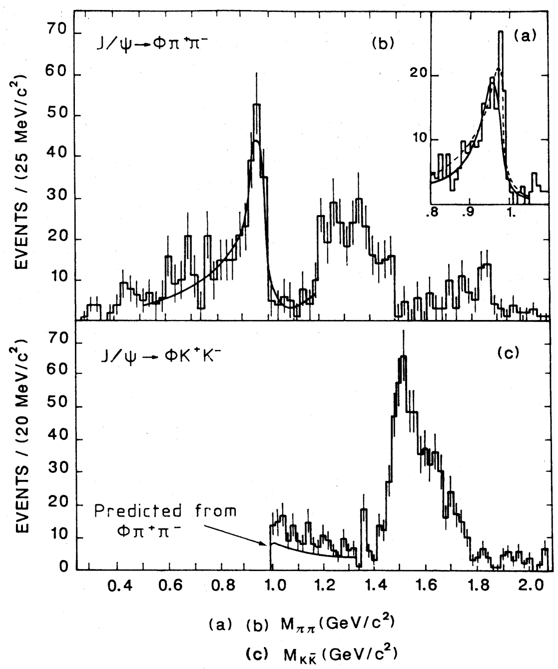

Figure 1: The DM2 data on (a), (b) $J/\psi \to \phi\pi^+\pi^-$ and (c) $J/\psi \to \phi K^+K^-$

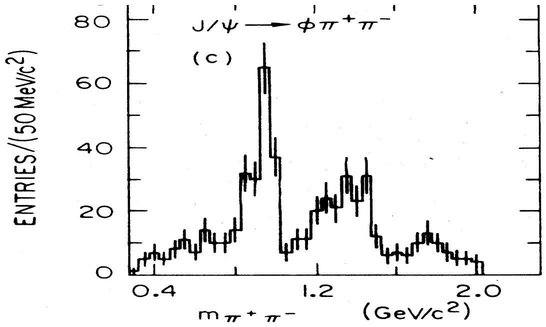

Figure 2: The MARK III data on $J/\psi \to \phi\pi^+\pi^-$

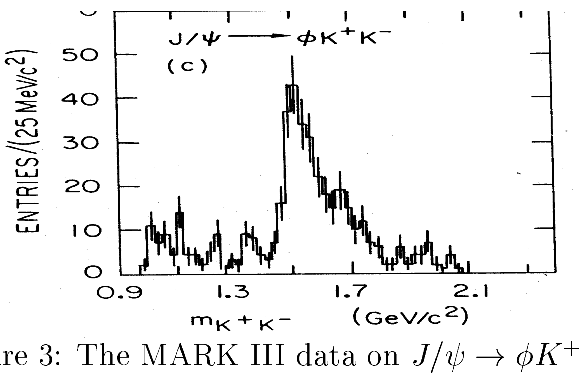

Figure 3: The MARK III data on $J/\psi \to \phi K^+K^-$

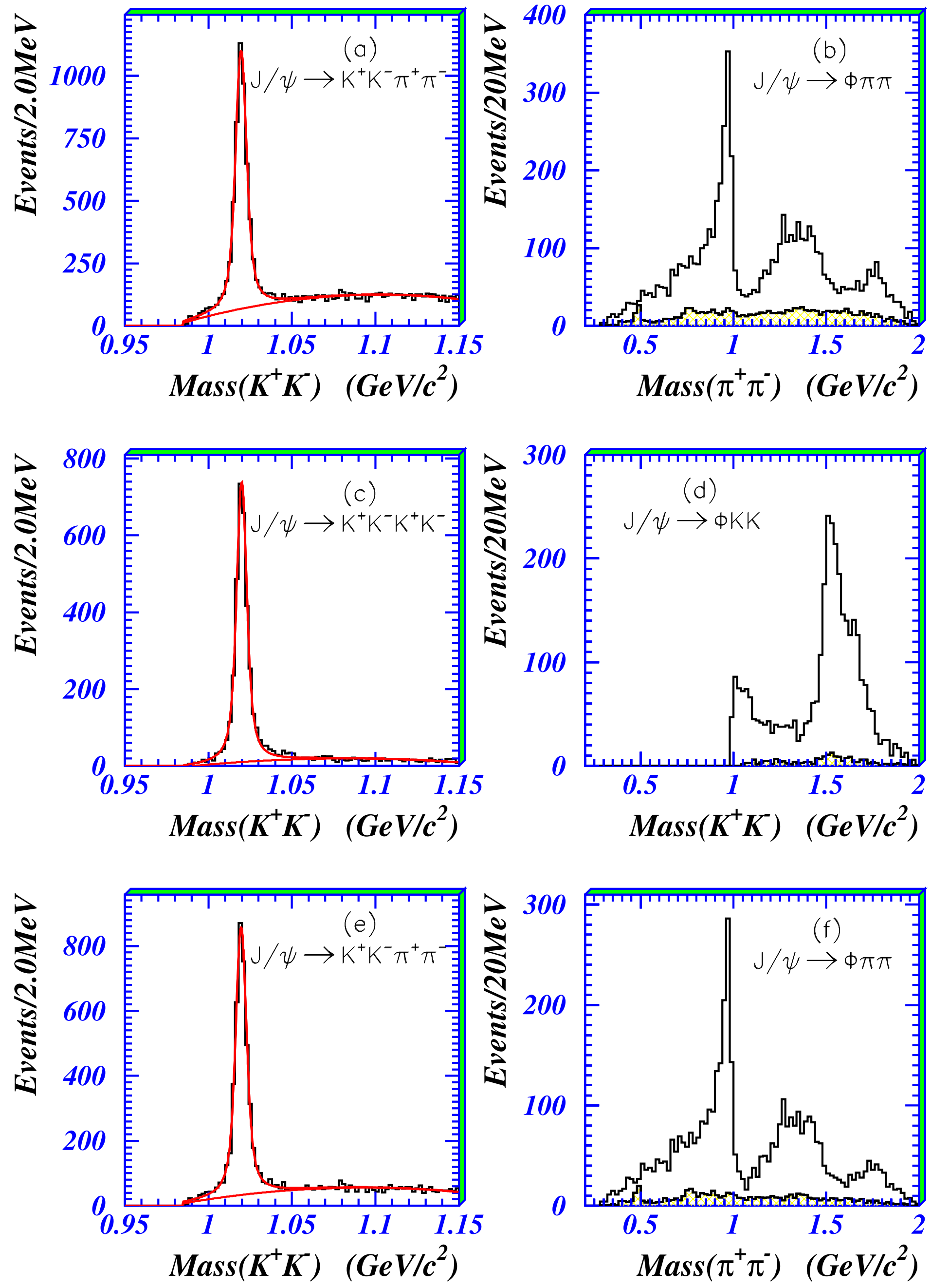

Figure 4: The K^+K^- invariant mass distributions for (a) $J/\psi \to K^+K^-\pi^+\pi^-$, (c) $J/\psi \to K^+K^-K^+K^-$. Curves show the fitted background and a Gaussian fit to the ϕ; (b) and (d) show mass projections for events selected within ± 15 MeV of the ϕ; the lower shaded histograms show background; (e) and (f) show mass projections after cutting events within ± 100 MeV of the central mass of $K^*(890)$.

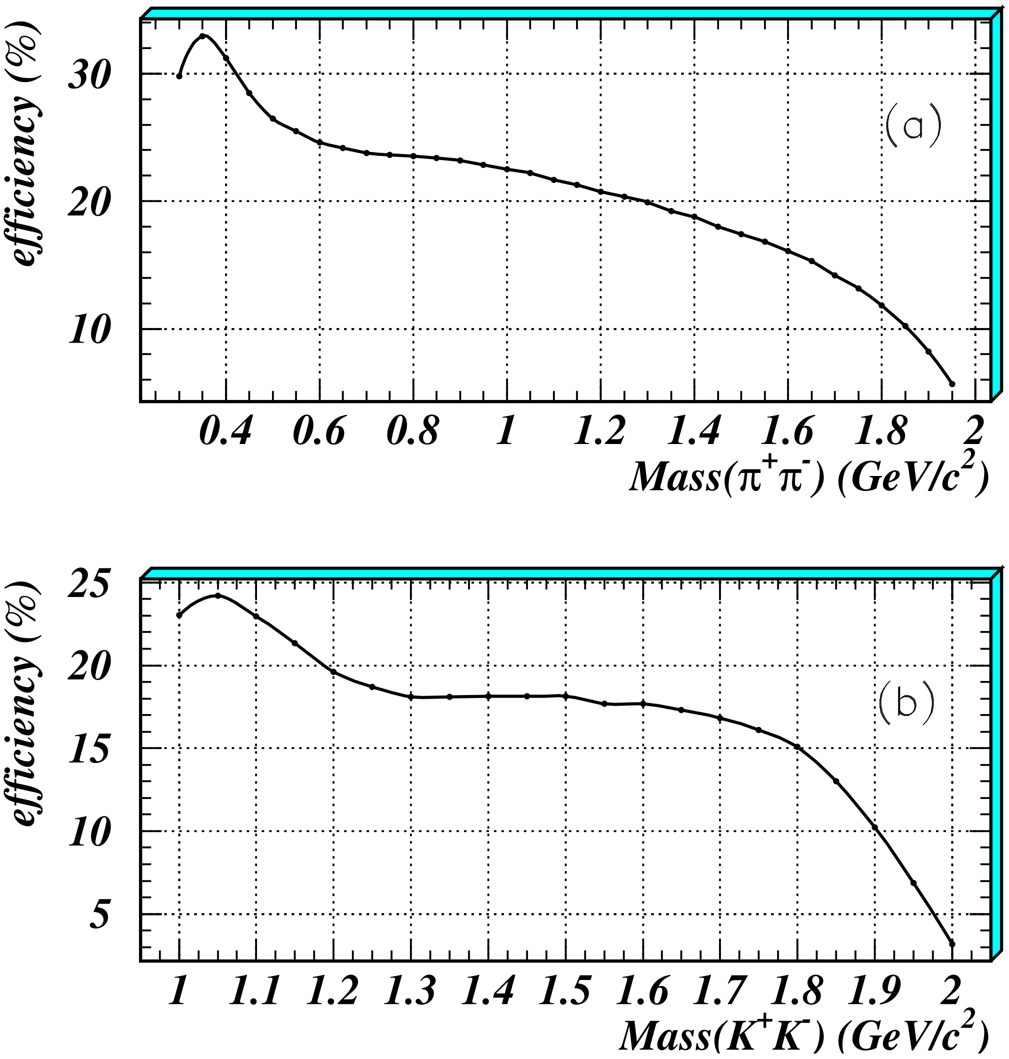

Figure 5: Efficiency for (a) $J/\psi \to \phi\pi^+\pi^-$ and (b) ϕK^+K^-

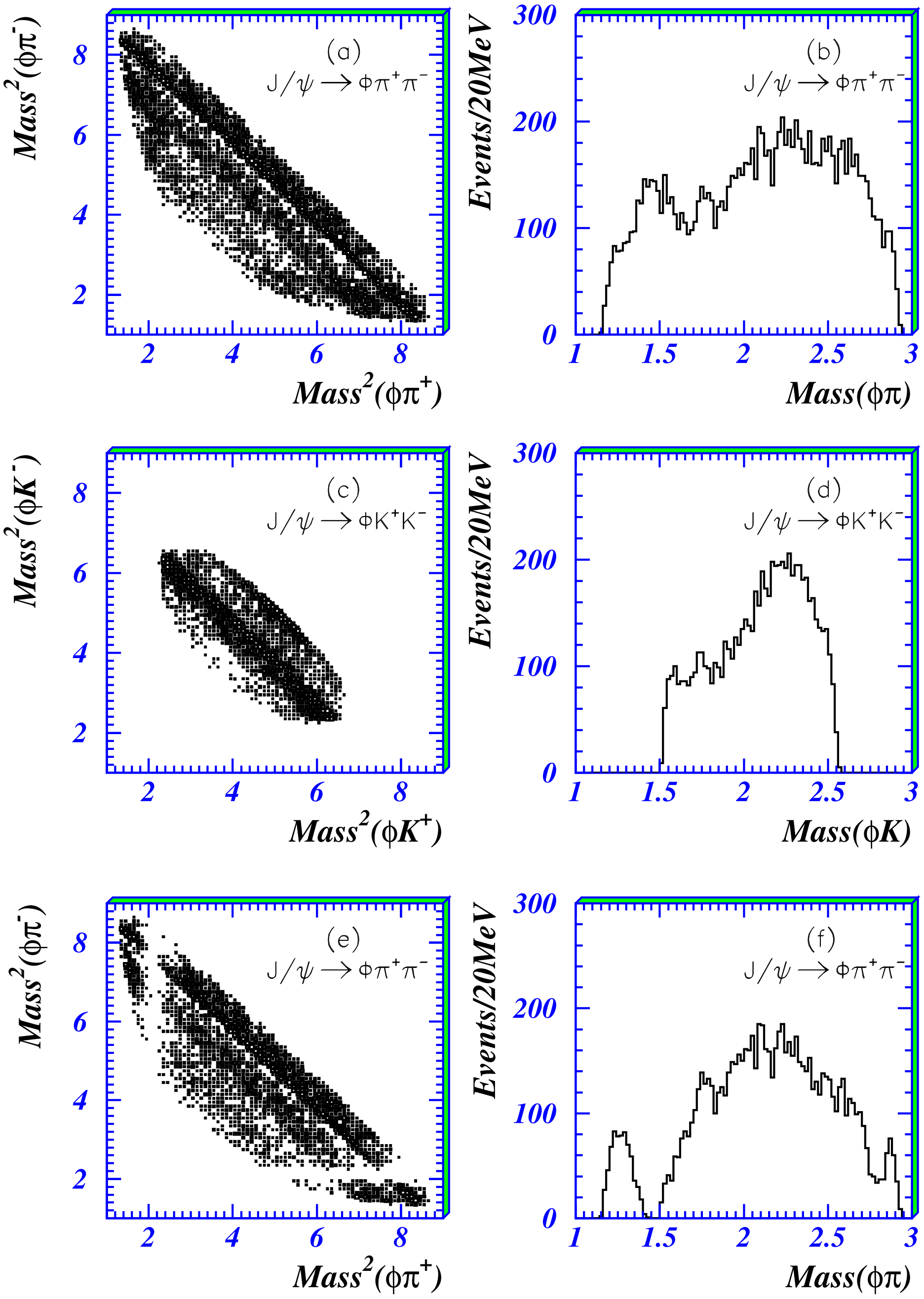

Figure 6: Dalitz plots for (a) $J/\psi \to \phi\pi^+\pi^-$, (c) $J/\psi \to \phi K^+K^-$; (b) and (d) show $\phi\pi$ mass projections; (e) and (f) show the result of cutting the $K^*(890)$.

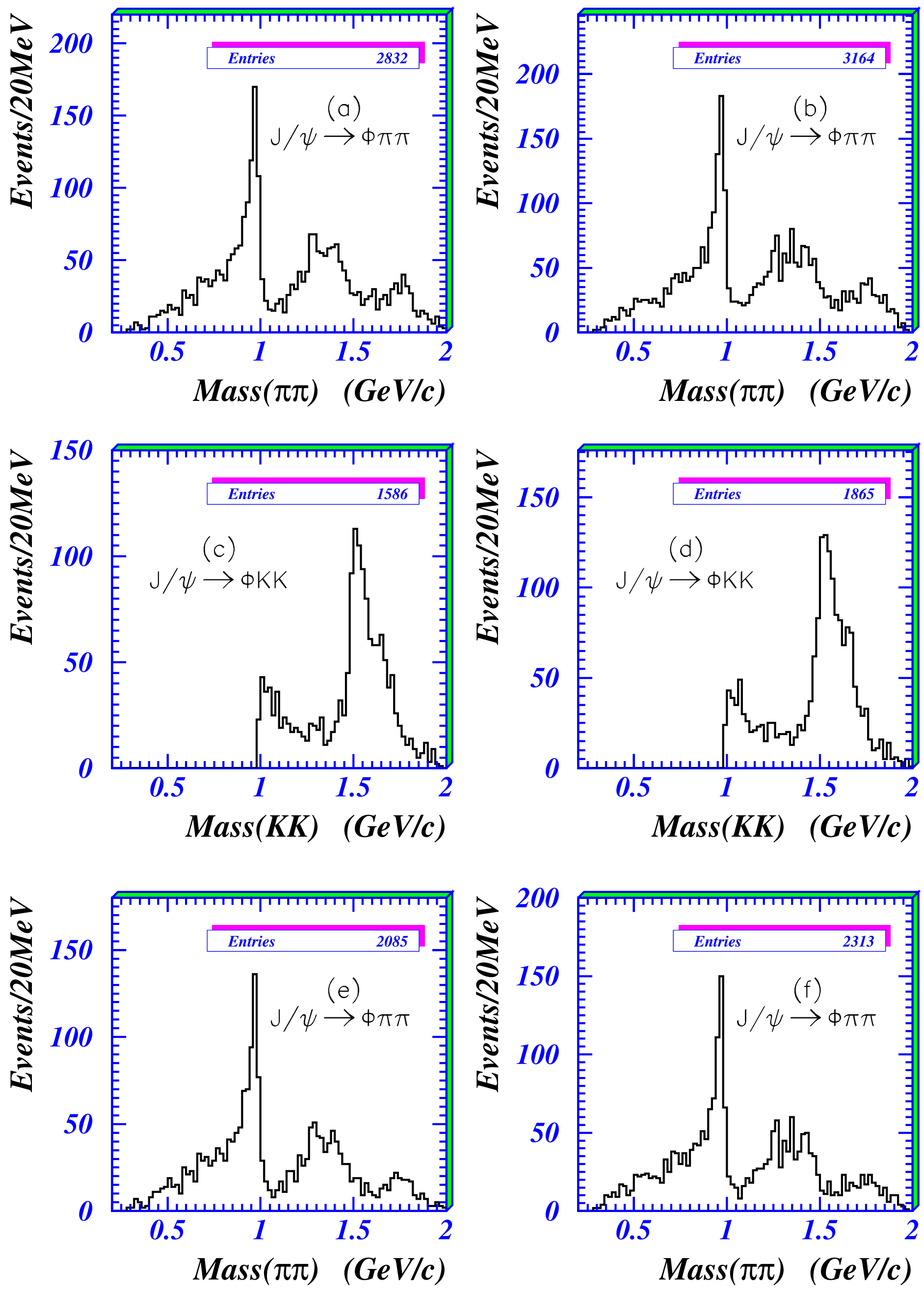

Figure 7: The first column show results from the first 24M event, the second column show results from thr last 26M. (a) and (b) M($\pi^+\pi^-$) from $J/\psi \to \phi\pi^+\pi^-$. (c) and (d) M($K^+K^-$) from $J/\psi \to \phi K^+K^-$. (e) and (f) as (a) and (b) after cutting out $K(890)$.

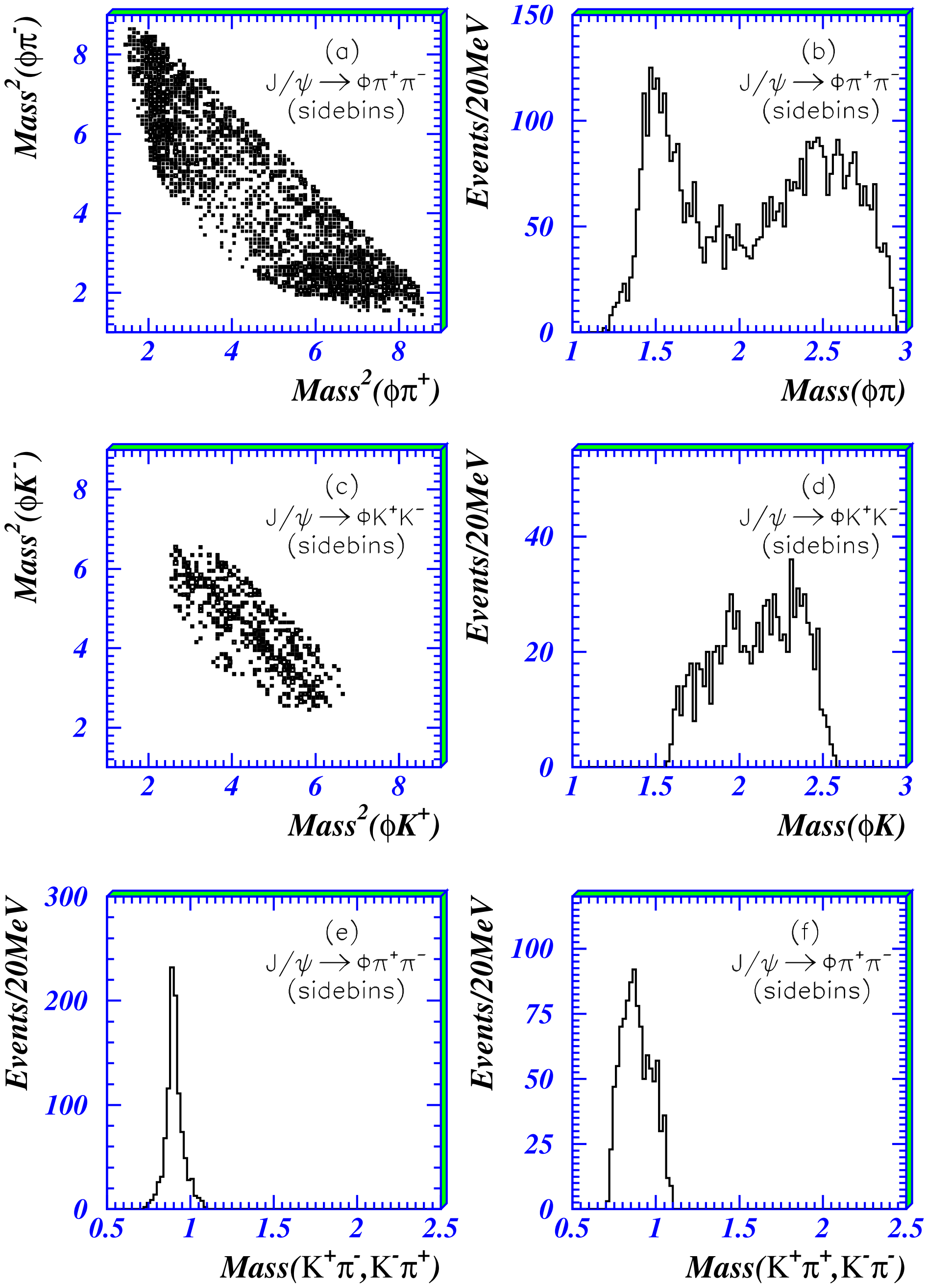

Figure 8: Dalitz plots for a sidebin to the ϕ with $M(K^+K^-) = 1.045$ to 1.09 GeV for (a) $K^+K^-\pi^+\pi^-$ data, (c) $K^+K^-K^+K^-$ data; (b) and (d) show projections against $\phi\pi^\pm$ and $\phi K^\pm$ mass; the mass distributions for (e) $M(K^+\pi^-)$ and $M(K^-\pi^+)$, (f) $M(K^+\pi^+)$ and $M(K^-\pi^-)$ for events from (a) in the $\phi\pi$ mass range 1400–1600 MeV.

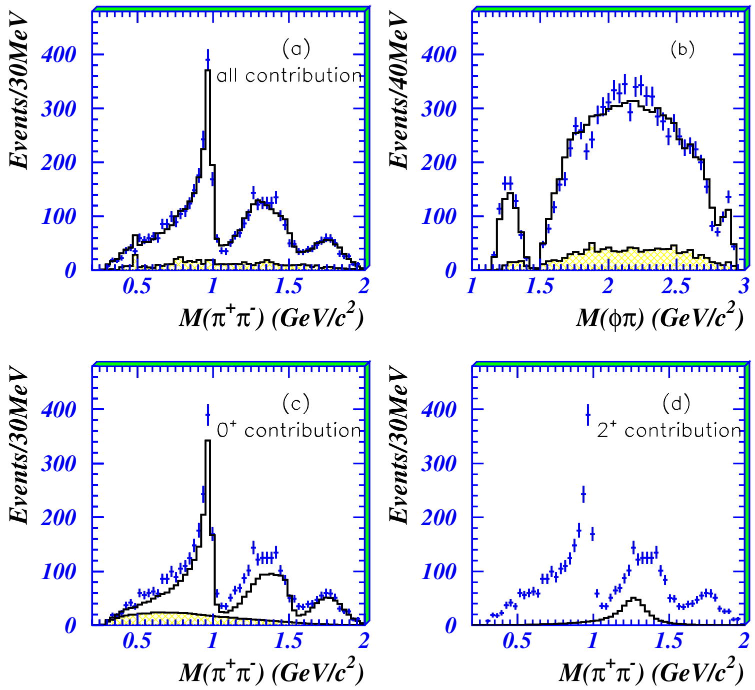

Figure 9: (a) and (b) Mass projections for $J/\psi \to \phi\pi^+\pi^-$ data after cutting $K^*(890)$ events; the upper histogram shows the maximum likelihood fit and the lower one shows background; (c) shows the f_0 contribution from the fit (full histogram) and the lower curve the σ contribution, (d) the f_2 contribution.

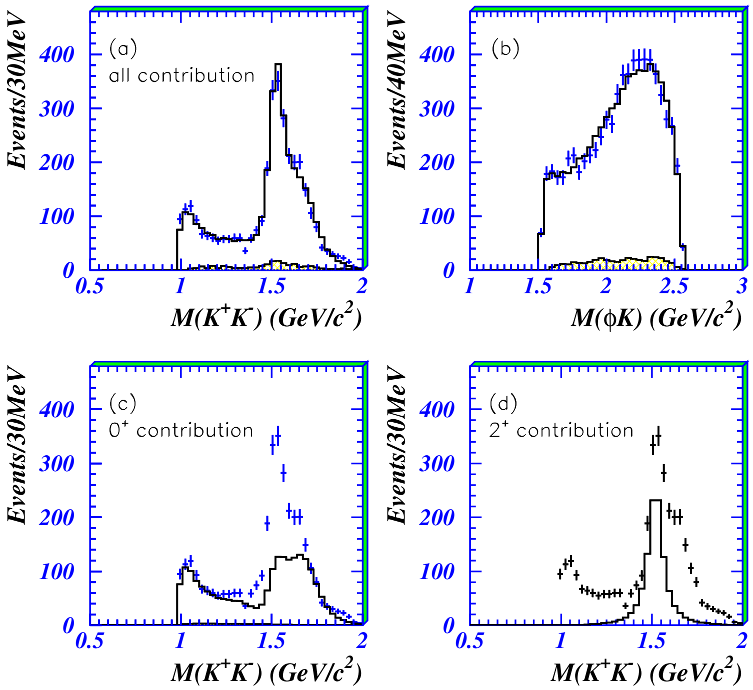

Figure 10: (a) and (b) Mass projections for $J/\psi \to \phi K^+K^-$ data, compared with histograms from the fit; (c) and (d) show f_0 and f_2 contributions.

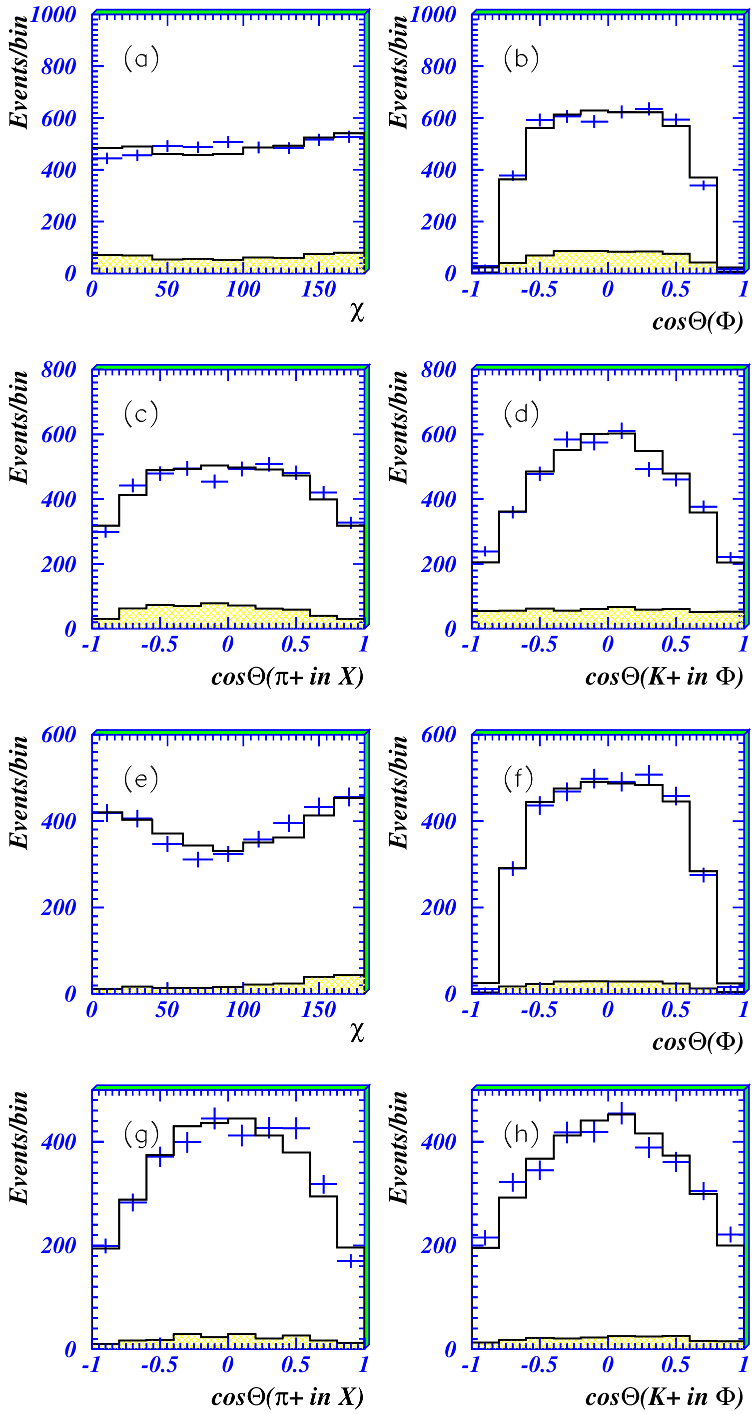

Figure 11: The angular distributions in $\phi\pi^+\pi^-$ data for (a) the angle χ between planes of decay of ϕ and f_0 (or f_2); the lower shaded histogram shows background; (b) the production angle of the ϕ, (c) the polar angle of the π^+ from f_J decay with respect to the direction of f_J in its rest frame, and (d) the corresponding angle of the K^+ in the rest frame of the ϕ; (e)–(h) show corresponding distributions in ϕK^+K^- data.

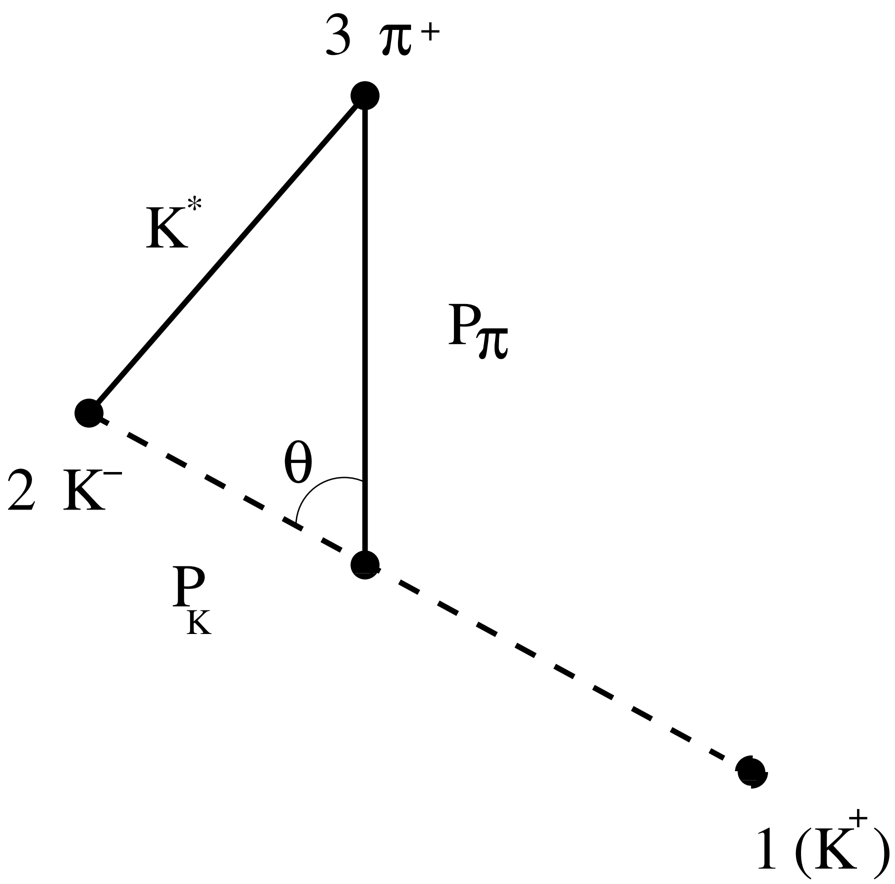

Figure 12: Kinematics of $K^+K^-\pi^+$